CARBON 47 (2009) 2898–2903

available at www.sciencedirect.com

ScienceDirect

journal homepage: www.elsevier.com/locate/carbon

# Enhanced optical absorption cross-section characteristics of multi-wall carbon nanotubes

C. Ni, P.R. Bandaru*

*Materials Science Program, Department of Mechanical and Aerospace Engineering, University of California, San Diego, Room 258, Engineering 2, 9500 Gilman Drive, MC 0411, La Jolla, CA 92093-0411, United States*

ARTICLE INFO

*Article history:*
Received 2 March 2009
Accepted 15 June 2009
Available online 21 June 2009

ABSTRACT

The optical absorption anisotropy of multi-walled carbon nanotubes (MWCNTs) has been quantitatively characterized through the determination of the absorbance and the degree of linear polarization. A model considering the orientation of the MWCNTs and the sensitivity to both co-polarized and cross-polarized radiation, through electric field depolarization effects, was used to understand the experimental results. The MWCNT optical absorption cross-sections for both the co-polarized radiation (~0.1 Å$^2$/atom) and the cross-polarized radiation (~0.05 Å$^2$/atom) were found to be much larger than for single-walled carbon nanotubes. Our results indicate the promise of MWCNTs for applications involving radiation absorption.



## 1. Introduction

The optical properties of both single-walled and multi-walled carbon nanotubes (CNTs) have been intensively studied for many applications [1] incorporating light emission [2], detection [3], and a wide electromagnetic absorption spectrum (60–2500 nm) [4–6]. The additional combination of high mechanical strength [7] together with appreciable electronic [8] and thermal conductivity [8,9] could also enable CNTs for coating materials, e.g., in pyroelectric detectors [10] and solar energy conversion.

A defining characteristic of the optical properties of CNTs arises from their anisotropic absorption due to their large aspect ratio/quasi one-dimensional topology. For example, it was seen that the absorption of electromagnetic radiation polarized parallel (co-/p-polarized) to the nanotube axis is larger than for the radiation polarized perpendicular (cross-/s-polarized) to the axis [11,12]. Such anisotropy can be quantitatively understood through the measurement of the optical absorption cross-section ($\sigma$), which is related to the ratio of the transmitted intensity ($I$) to the incident intensity ($I_0$), through $I = I_0 \exp(-n\sigma t)$ for a certain thickness ($t$) of the material and material/CNT density ($n$). Note that the absorption coefficient is defined here as $n\sigma$, while the absorbance, $\Lambda$, is $n\sigma t$. The transmittance ($T$) is defined and measured through $I/I_0$.

In this paper, we report on the optical absorption cross-section anisotropy ($\sigma_{\|}/\sigma_{\perp}$; $\sigma_{\|}$ for co-polarization and $\sigma_{\perp}$ for cross-polarization) for multi-walled CNTs (MWCNTs) as a function of nanotube diameter. Such measurements and quantitative determination, in addition to being of scientific interest, can be used to interpret the degree of CNT alignment [12]. It was seen that in comparison to the single-walled CNTs (SWCNTs) [12], MWCNTs have much higher absorption cross-sections [13] with a dominant contribution from the outermost layers.

## 2. Experimental procedure

Mats comprising vertically aligned MWCNTs were synthesized on quartz substrates via thermal chemical vapor deposition (CVD), using a 2–7 nm thick electron-beam evaporated Fe catalyst film. The CNT growth was carried out using a mixture of $C_2H_2$ (99.96%) and Ar (99.999%) with flow rates of

* *Corresponding author:* Fax: +1 858 534 5698.
E-mail address: pbandaru@ucsd.edu (P.R. Bandaru).
0008-6223/$ - see front matter 
doi:10.1016/j.carbon.2009.06.038

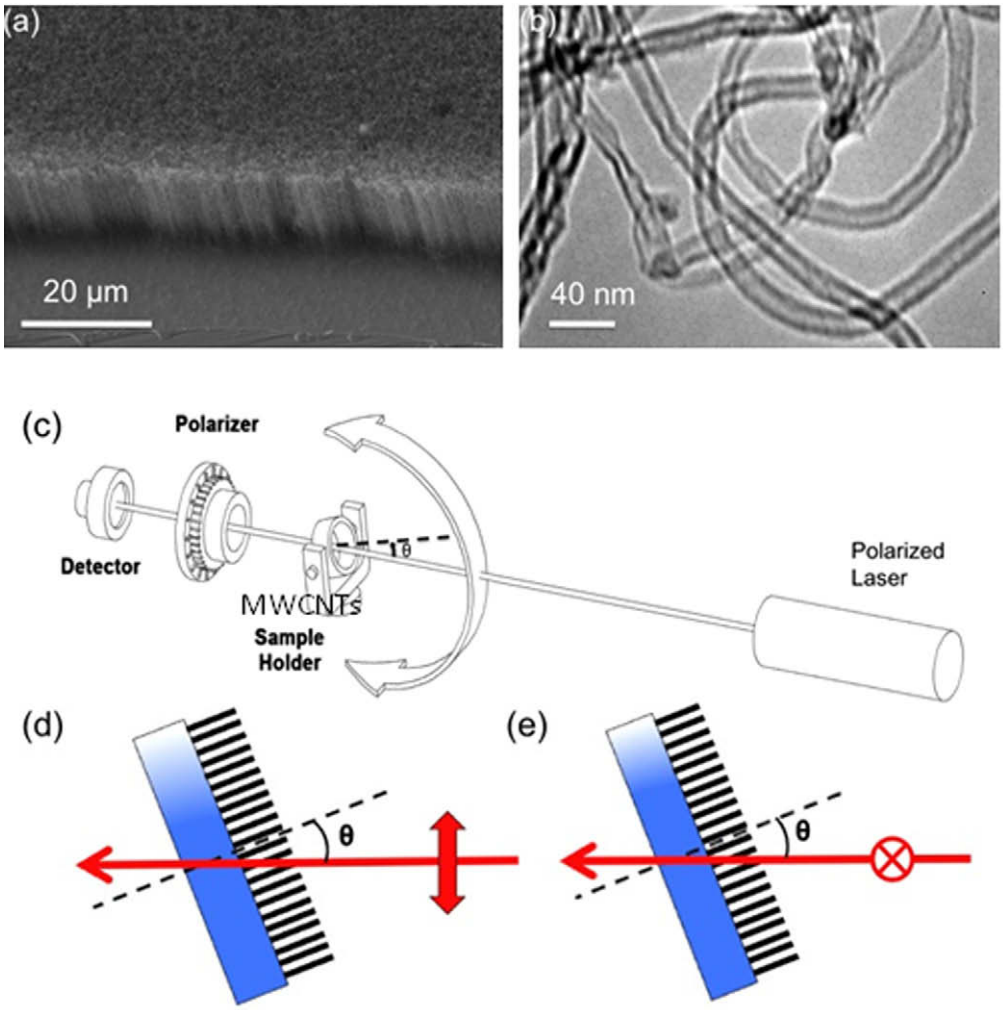


**Fig. 1 – (a) SEM and (b) TEM images of synthesized MWCNT ensembles, (c) schematic of experimental setup of the absorption measurements, in the (d) co-polarized, and (e) cross-polarized configurations.**

30 sccm and 400 sccm, respectively. SEM images of the nanotube film revealed a uniformly aligned MWCNT ensemble (Fig. 1a) with an average height, $L \sim 15$ μm, and diameter in the range of 5–20 nm (Fig. 1a).

The optical characterization was implemented mainly through the experimental setup illustrated in Fig. 1c. Polarized light (473 nm/633 nm) from linearly polarized lasers was shone onto the MWCNT sample (at an angle $\theta$; $0 < \theta < \pi/2$). The optical path length, $t$, is hence equal to $L/(\cos\theta)$. The measurements were conducted both in the *co-polarized* (electric field parallel to the plane of incidence (Fig. 1d) – and *cross-polarized* (electric field perpendicular to the plane of incidence (Fig. 1e) – configurations. The transmitted intensity was analyzed by a polarizer, before being collected by a photodetector (Thorlabs DET 110).

## 3. Results and discussion

### 3.1. *Absorbance characteristics of MWCNTs*

Fig. 2a shows the measured transmitted intensity ($I$) dependence of the MWCNT samples for co- and *cross-polarized* radiation of wavelengths 473 and 633 nm as a function of substrate tilt, $\theta$. In the figure caption, we use arbitrary units for $I$ as neutral density filters were used (to bring the signals to the measurable range of the lock-in amplifier). A higher transmission was observed for the *cross-polarized* radiation compared to the *co-polarized* case, due to electric-field-induced *depolarization* from the nanotube cross-section in the latter which reduces the dynamical conductivity and lowers optical absorption [14]. A reduced transmission for shorter wavelength radiation was also noted [12,13] and could arise from increased propensity for surface and bulk $\pi$-plasmon excitations [15]. The absorbance ($\Lambda$) was calculated from the ratio of the transmitted to the incident intensity, through $I = I_0 \exp(-\Lambda)$, and is plotted in Fig. 2b. The effective thickness, $t$, in $\Lambda$ ($=n\sigma t$) was normalized to $t = L/\cos\theta$, to account for the substrate tilt. While in the *cross-polarized* case, the absorbance, $\Lambda^{cr}$, was largely independent of $\theta$ – as expected from Fig. 1d, a $\sin^2\theta$ variation for the *co-polarized* absorbance, $\Lambda^{co}$ (Fig. 2c) was observed. It was noted that the $\Lambda^{co}$ for 473 nm was lower at larger $\theta$, compared to the 633 nm case, due to greater light leakage. Such a dependence was justified when the component of the electric field parallel to the nanotube,

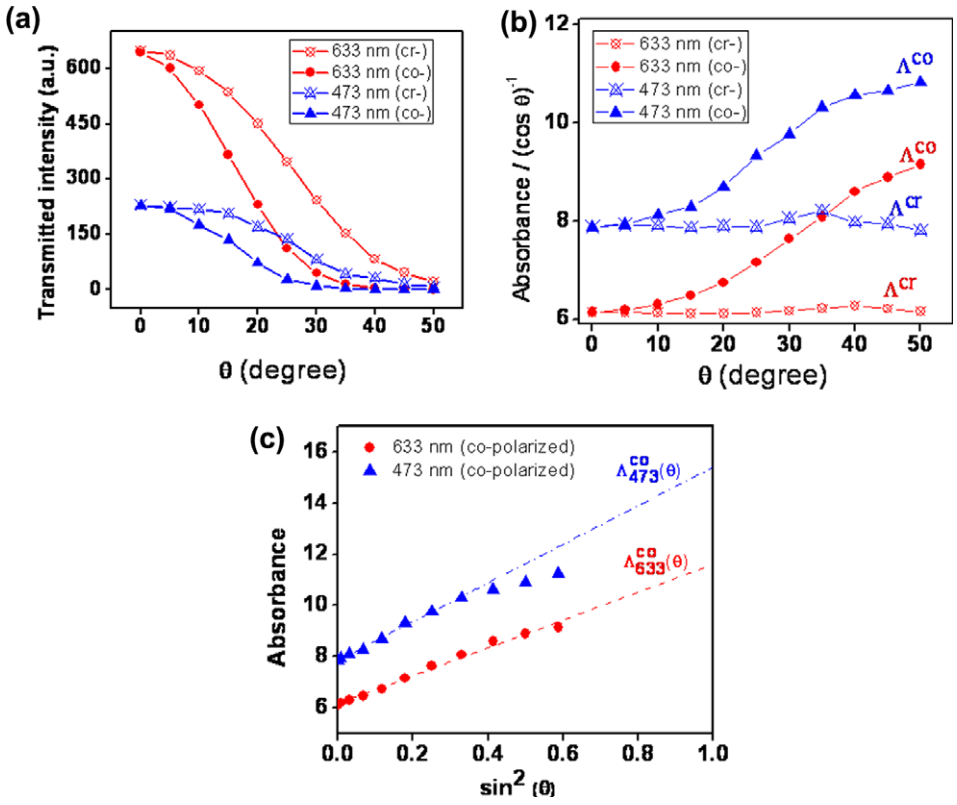


**Fig. 2 – (a) Transmitted intensity of 633 and 473-nm radiation for the *co-* (co-) and *cross-* (cr-) polarized configurations. (b) A higher absorbance ($\Lambda$), normalized to the effective path length, by $(\cos\theta)^{-1}$, is indicated for the 473-nm radiation and the *cross-polarized* ($\Lambda^{cr}$) configuration, (c) $\Lambda^{co}$ is found to be proportional to $\sin^2\theta$.**

i.e., $E^{co\prime} = E^{co} \sin\theta$ was considered [13] and the transmitted intensity (which is proportional to $\Lambda^{co}$) related to the square of the electric field, through $|E^{co\prime}|^2$. The value of the $\Lambda^{co}$ at $\theta = 0°$ [$\Lambda^{co}(0°)$] gave the absorbance for the *cross-polarized* configuration while through extrapolating the measured absorbance to $\theta = 90°$, i.e., $\Lambda^{co}$ ($\theta = 90°$), the absorbance for *co-polarized radiation* was noted. The corresponding values, for both 473 and 633 nm wavelengths, are listed in Table 1. It was then inferred, for example, that at 473 nm, the nanotube absorption for *co-polarized* radiation was ~900 times (related to $\exp[\Lambda^{co}-\Lambda^{cr}] = \exp[14.9-8.1] = e^{6.8}$) larger than in the *cross-polarized* case. While reflectance could be an issue, it is more important at larger angles. Consequently, we have used small incidence angles (<40°) for our measurements and analyses (e.g., see Fig. 2c, where only the linear part of the graph has been used). We have estimated a maximum reflectance of <6% for co-polarized light and a reflectance of <10% for cross-polarized light [16].

With a *perfectly aligned* nanotube mat, the absorption cross-sections $\sigma$, for either the parallel ($\sigma_{\|}$) or perpendicular ($\sigma_{\perp}$) radiation configuration, could be derived through $\Lambda_{\|} = n\sigma_{\|}t$ and $\Lambda_{\perp} = n\sigma_{\perp}t$, respectively, given a known CNT density, $n$, and $t$. However, such an assumption was unrealistic as we observed through scanning electron microscopy (SEM) observations (Fig. 1a) that the synthesized MWCNTs were not *exactly* vertical to the substrate, but have a range of orientations.

**Table 1 – Absorbance ($\Lambda$), at 473 and 633 nm for co-polarized [$\Lambda^{co}$ (90°)], and cross-polarized [$\Lambda^{cr}$ (0°)] incident radiation.**

| $\lambda$ (nm) | Absorbance | |
|---|---|---|
| | $\Lambda^{co}$ (90°) = $\Lambda'_{\|}$ | $\Lambda^{co}$ (0°) = $\Lambda'_{\perp}$ |
| 473 | 14.9 | 8.1 |
| 633 | 11.7 | 6.1 |

### 3.2. *Influence of the degree of alignment of MWCNT on transmitted intensity*

The transmitted intensity, $I$, is a function of both (i) polarization angle, $\alpha$, and (ii) the overall alignment of the CNTs. For (i), $I(\alpha) = I_0 \sin^2\alpha$, where $\alpha$ was the angle between the radiation polarization direction and the nanotube axis. The electric field ($E$) of the incident radiation on a MWCNT is described through $E = E_{\|} + E_{\perp}$ ($E_{\|} = \vec{i}\,|E|\cos(\alpha)$ and $E_{\perp} = \vec{j}\,|E|\sin(\alpha)$ and where $I_0 = |E|^2$. Since it was previously determined (Section 3.1) that the absorption of the *co-polarized* radiation was orders of magnitude larger than the *cross-polarized* radiation, the total *transmitted* electric field was expected to be close to $E_{\perp}$, i.e., $E \sim E_{\perp}$. With a *perfectly* aligned CNT sample it was then expected that $I(0°) = I(180°) = 0$, with

minimum transmission (related to $\mathbf{E}_\perp$) while $I(90°)[=I(270°)]$ is related to maximum transmission.

As previously outlined, the *co-* and *cross-polarized* absorbances, $\Lambda_\parallel$ and $\Lambda_\perp$ are strictly defined for perfectly oriented nanotubes, i.e., $\langle\varphi\rangle = 0$ where $\varphi$ is the polar angle between the nanotube axis and substrate normal as defined in Fig. 3a. For a more disordered orientation, i.e., $\langle\varphi\rangle \neq 0$, the degree of CNT alignment should be considered. Consequently, the absorbance ($\Lambda$) would be modified to, say $\Lambda'_\parallel$ and $\Lambda'_\perp$, for the *co-* and *cross-polarized* case, respectively.

To model the CNT misalignment, we assumed a statistical Gauss–Boltzmann distribution $P(\varphi)$ [17], of the type:

$$P(\varphi) = \frac{\exp(-A \cdot \sin^2\varphi)}{\int_{-1}^{1} \exp(-A \cdot \sin^2\varphi) d(\sin\varphi)}$$

$P(\varphi)$ has a maximum probability at $\varphi = 0°$, as shown in Fig. 3a. A is a parameter, which tends to infinity for perfectly aligned CNT mats and can be used to characterize alignment. The parameter A was then determined to be ~80 for our particular MWNT ensemble by comparing the measured transmitted intensity to a simulated intensity, and was obtained by convoluting $P(\varphi)$ at various values of A with $\langle I(\alpha)\rangle$ (Fig. 3b).

### 3.3. Order parameter and modified optical absorption cross-sections

Having determined the appropriate $P(\varphi)$ we determined an order parameter [12,18] S, $(0 < S < 1)$ defined through: $S = \int_{-1}^{1} P(\varphi)(3\cos^2\varphi - \frac{1}{2}) d(\cos\varphi)$. $S = 0$ corresponds to a completely random/isotropically aligned CNT ensemble while $S = 1$ corresponds to perfect vertical alignment. We then estimated, from the above expression, an $S \sim 0.82$. The effect of such a finite S would be to modify the cross-sections, from $\sigma_\parallel$ and $\sigma_\perp$ to $\eta_\parallel$ and $\eta_\perp$, respectively. Consequently, we express $\eta_\parallel = a\ S + b$, and $\eta_\perp = c\ S + d$, with the constraint that the net sum, $\eta_\parallel + 2{\cdot}\eta_\perp$ is a constant (*a*, *b*, *c*, and *d*, are constants) which follows from the consideration that such a sum which is characteristic of an isotropic/unaligned sample is unchanged from one sample to another [12]. The modified cross-sections ($\eta_\parallel$ and $\eta_\perp$) were then derived from the *measured* absorbance ($\Lambda'_\parallel$ and $\Lambda'_\perp$) (see Table 1), i.e., through $\eta_\parallel = \frac{\Lambda'_\parallel}{nt}$ and $\eta_\perp = \frac{\Lambda'_\perp}{nt}$. The CNT density, *n*, was estimated to be $\sim 1.1 \times 10^{-3}$ mol/cm$^3$ – assuming 20 nm diameter MWNTs arranged ~200 nm apart through the SEM observations made on samples shown in Fig. 1a.

The *true absorption cross-sections* ($\sigma_\parallel$ and $\sigma_\perp$) were then calculated from the following equations [12]:

$$\eta_\parallel = \frac{2}{3}(\sigma_\parallel - \sigma_\perp)S + \frac{1}{3}(\sigma_\parallel + 2\sigma_\perp)$$

$$\eta_\perp = -\frac{1}{3}(\sigma_\parallel - \sigma_\perp)S + \frac{1}{3}(\sigma_\parallel + 2\sigma_\perp)$$

These values along with the degree of linear polarization (DLP) = $\frac{\sigma_\parallel - \sigma_\perp}{\sigma_\parallel + \sigma_\perp}$, are listed in Table 2. The values previously obtained [13] for SWCNTs were also tabulated for comparison. It was noted that the optical *absorption cross-sections* of the multi-walled CNTs were an order of magnitude larger than those of SWCNTs. However, the DLP is approximately 35% smaller.

### 3.4. Relationship of the degree of linear polarization to nanotube diameter

As the absorption cross-sections and the DLP seem to be related to the nanotube diameter (e.g., $DLP_{SWCNT} > DLP_{MWCNT}$, as in Table 2), it would be of interest to understand such dependencies in more detail. For this purpose, we measured the absorbance ($\Lambda^{co}$ and $\Lambda^{cr}$) of MWCNTs of different diame-

**Table 2 – The co- ($\sigma_\parallel$) and cross- ($\sigma_\perp$) polarized absorption cross-sections and the degree of linear polarization (DLP) for MWCNTs and SWCNTs.**

| Nanotube | Wavelength (nm) | $\sigma_\parallel$ (Å$^2$/atom) | $\sigma_\perp$ (Å$^2$/atom) | DLP |
|---|---|---|---|---|
| MWCNT | 473 | 0.117 | 0.062 | 0.31 |
| | 633 | 0.098 | 0.047 | 0.35 |
| SWCNT | 473 | 0.029 | 0.007 | 0.60 |
| | 633 | 0.025 | 0.005 | 0.65 |

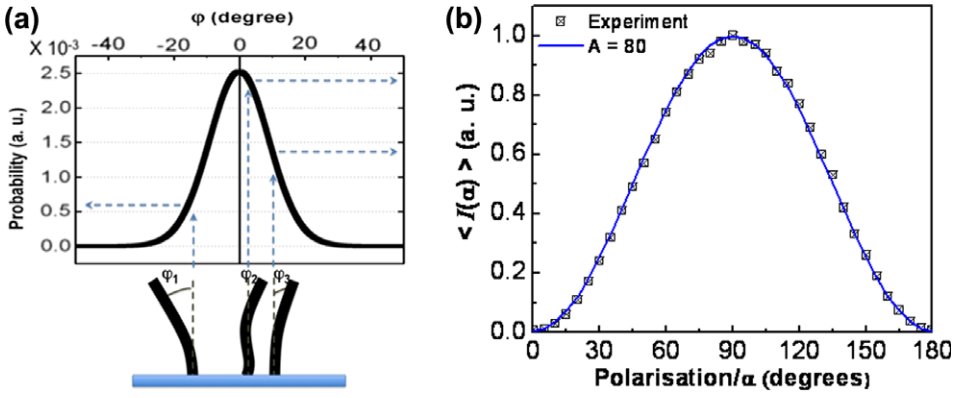


**Fig. 3 – (a) The distribution/degree of alignment (through the angle $\varphi$) of the synthesized MWCNTs was modeled to follow a Gauss–Boltzmann type distribution, $P(\varphi)$. (b) The variation of the experimentally measured transmitted intensity with the angle of polarization, $\alpha$, is in excellent agreement with the simulated intensity obtained by convoluting $P(\varphi)$ (with an $A \sim 80$) with the expected transmission.**

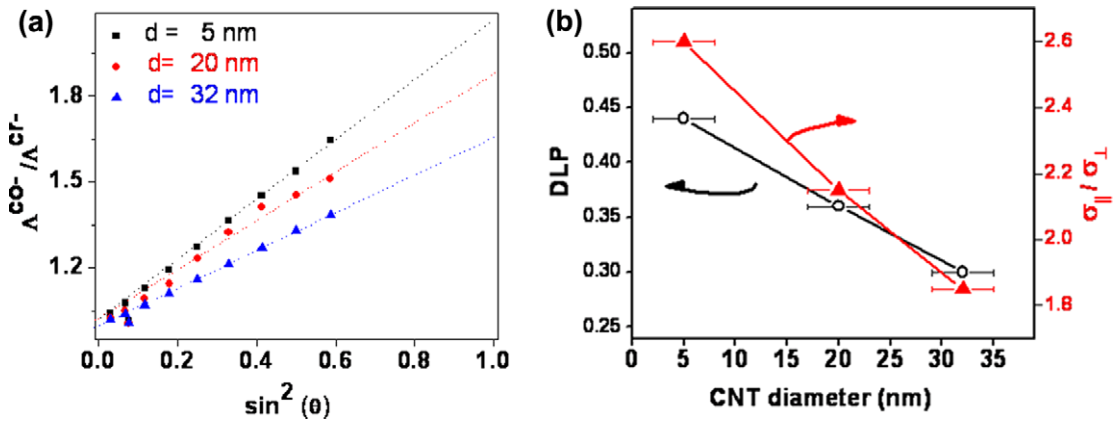


**Fig. 4 – (a) The absorbance ratio ($\Lambda^{co}/\Lambda^{cr}$) increases proportionately with the MWCNT diameter (*d*). *The straight lines are a guide to the eye.* (b) The degree of linear polarization (DLP) and the absorption cross-section anisotropy ($\sigma_{\parallel}/\sigma_{\perp}$) as a function of the nanotube diameter.**

ters ($d \sim 5$, 20, and 32 nm) grown from catalyst (Fe) films of different thicknesses (1.2, 2.8, and 5.5 nm, respectively). Fig. 4a, indicates, as was previously observed, that the absorbance anisotropy ($=\Lambda^{co}/\Lambda^{cr}$) varies with $\sin^2\theta$ (c.f., Fig. 2c) and decreases with increasing catalyst film thickness/nanotube diameter. The DLP and the absorption cross-section anisotropy ($=\sigma_{\parallel}/\sigma_{\perp}$) exhibit a similar trend (Fig. 4b).

While the correlation between the optical absorption and tube diameter of CNT has not yet been resolved [19], the effects of the depolarization electric field ($\mathbf{E}_d$) were used to give a qualitative interpretation of the correlation between absorption cross-section anisotropy ($\sigma_{\parallel}/\sigma_{\perp}$) and the tube diameter (*d*). For *cross-polarized* radiation, the depolarization effect was relaxed as tube diameter increases (i.e., $\mathbf{E}_d \sim 1/d$), due to a reduced local charge density resulting in $\sigma_{\perp}$ increasing with an increase in *d* through $\sigma_{\perp} \sim 1/\mathbf{E}_d \sim d$. On the other hand, this depolarization effect does not occur for *co-polarized* radiation as the electric field/polarization is now parallel to the long axis of the CNT, which leads to $\sigma_{\parallel}$ independent of $\mathbf{E}_d$. The absorption cross-section ($\sigma_{\parallel}/\sigma_{\perp} \sim \mathbf{E}_d \sim 1/d$) was then derived to be inversely proportional to *d*. Since a MWCNT can be thought of as being composed of many SWCNTs arranged coaxially would be easy to attribute $\sigma_{\parallel}$ of a MWCNT to the summation of those of the constituent SWCNTs, leading to $\sigma_{\parallel}$ increasing with *d*. However, if a MWCNT is considered metallic [20], the $\sigma_{\parallel}$ of a MWCNT would then only be due to the external layer due to screening effects [21]. Such correlation could be supported by a previous study on the thermal properties of MWCNTs [22], which indicated weak inter-wall coupling in MWCNT.

## 4. Conclusions

In summary, we have quantitatively determined, for the first time, the absorption cross-sections for *co-polarized* (light polarization parallel to the nanotube axis) and *cross-polarized* (light polarization perpendicular to the nanotube axis) radiation for multi-walled CNTs. In the experimental measurements, the orientation and misalignment of the nanotubes was also considered. It was seen that the measured cross-sections (~0.1 Å$^2$/atom) are *much larger* than those previously determined for single-walled CNTs. Additionally, the *co-polarized* cross-section is larger by a factor of two compared to the *cross-polarized* absorption cross-section. However, the degree of linear polarization (DLP) was seen to be smaller for the MWCNT ensembles. The reduction of the depolarization electric field perpendicular to the CNTs with increasing diameter and the consequent increased absorption could be responsible for the reduced DLP. These results indicate that while MWCNTs are inferior nanoscale polarizing elements, their increased absorption cross-sections could be utilized for applications involving radiation detection and absorption.

## Acknowledgements

We gratefully acknowledge support from the National Science Foundation (Grants ECS-05-08514 and DMI-0304019) and the Office of Naval Research (Award Number N00014-06-1-0234).

## REFERENCES

[1] Bandaru PR. Electrical properties and applications of carbon nanotube structures. J Nanosci Nanotechnol 2007;7:1239–67.
[2] Chen J, Perebeinos V, Freitag M, Tsang J, Fu Q, Liu J, et al. Bright infrared emission from electrically induced excitons in carbon nanotubes. Science 2005;310:1171–4.
[3] Freitag M, Martin Y, Misewich JA, Martel R, Avouris P. Photoconductivity of single carbon nanotubes. Nano Lett 2003;3:1067–71.
[4] Yang Z, Ci L, Bur A, Lin S, Ajayan P. Experimental observation of an extremely dark material made by a low-density nanotube array. Nano Lett 2008;8:446–51.
[5] Taft E, Philipp H. Optical properties of graphite. Phys Rev B 1965;138:197–202.
[6] Longe P, Bose S. Collective excitations in metallic graphene tubules. Phys Rev B 1993;48:18239–43.
[7] Treacy MMJ, Ebbesen TW, Gibson JM. Exceptionally high Young's modulus observed for individual carbon nanotubes. Nature 1996;381:678–80.
[8] Zhou X, Park J-Y, Huang S, Liu J, McEuen PL. Band structure, phonon scattering, and the performance limit of single-

walled carbon nanotube transistors. Phys Rev Lett 2005;95:146805-1–4.
[9] Kim P, Shi L, Majumdar A, McEuen PL. Thermal transport measurements of individual multiwalled nanotubes. Phys Rev Lett 2001;87:215502-1–4.
[10] Theocharous E, Deshpande R, Dillon A, Lehman L. Evaluation of a pyroelectric detector with a carbon multiwalled nanotube black coating in the infrared. Appl Opt 2006;45:1093–7.
[11] Shoji S, Suzuki H, Zaccaria R, Sekkat Z, Kawata S. Optical polarizer made of uniaxially aligned short single-wall carbon nanotubes embedded in a polymer film. Phys Rev B 2008;77:153407-1–4.
[12] Islam MF, Milkie DE, Kane CL, Yodh AG, Kikkawa JM. Direct measurement of the polarized optical absorption cross section of single-wall carbon nanotubes. Phys Rev Lett 2004;93(3):037404-1–4.
[13] Murakami Y, Einarsson E, Edamura T, Maruyama S. Polarization dependent optical absorption properties of single-walled carbon nanotubes and methodology for the evaluation of their morphology. Carbon 2005;43:2664–76.
[14] Aijiki H, Ando T. Aharanov–Bohm effect in carbon nanotubes. Physica B (Amsterdam) 1994;201:349–52.
[15] Reed B, Sarikaya M. Electronic properties of carbon nanotubes by transmission electron energy-loss spectroscopy. Phys Rev B 2001;64:195404-1–13.
[16] Saleh BEA, Teich MC. Fundamentals of photonics. 2nd ed. Hoboken, NJ: John Wiley and Sons; 2007.
[17] Fujiwara M. Magnetic orientation and magnetic properties of a single carbon nanotube. J Phys Chem A 2001;105(18): 4383.
[18] Chaikin PM, Lubensky TC. Principles of condensed matter physics. New York: Cambridge University Press; 1995.
[19] Jost O, Gorbunov A, Pompe W, Pichler T, Friedlein R, Knupfer M, et al. Diameter grouping in bulk samples of single-walled carbon nanotubes from optical absorption spectroscopy. Appl Phys Lett 1999;75:2217–9.
[20] Martel R, Schmidt T, Shea HR, Hertel T, Avouris P. Single- and multi-wall carbon nanotube field-effect transistors. Appl Phys Lett 1998;73:2447–9.
[21] Ando Y, Zhao X, Shimoyama H, Sakai G, Kaneto K. Physical properties of multiwalled carbon nanotubes. Int J Inorg Mater 1999;1:77–82.
[22] Yi W, Lu L, Zhang DL, Pan ZW, Xie SS. Linear specific heat of carbon nanotubes. Phys Rev B 1999;59:R9015–8.